DOI:10.24996/ijs.2018.59.4A.11

ISSN: 0067-2904

Structure and Morphological Properties of In_2O_3 Nanostructure Prepared by Pulse Laser Ablation Method

Sariya D.AL. ALgawi[1], Wafaa K. Khalef[1], Sura R.Mohammed*[2]
[1]Applied Science Department, University of Technology, Baghdad, Iraq
[2]Ministry of Science & Technology, Iraqi National Monitoring Authority (INMA) , Baghdad, Iraq

Abstract

A colloidal indium oxide (In_2O_3) nanoparticles (NPs) were synthesized pulsed laser ablation (PLA) of indium plate placed on the bottom of the quartz vessel containing (3ml) of pure ethanol. The influence laser energy on the properties of the formed nano-particles were characterized by using atomic force microscopy (AFM), X-ray diffraction (XRD), Ultraviolet Visible (UV-Vis) technique, and electrical properties measurements. The XRD revealed the crystallization structure of In_2O_3 nanoparticles and all the films having preferential orientation along (222) plane and intensity increases with increasing laser energy, The UV–Visible spectrum of the colloidal nanoparticles maximum absorbance show around the UV region, which indicates the formation of In_2O_3 nanoparticles with energy gap about (3.6, 3.8 and 3.9) eV for different laser energy's (150, 300 and 500) mj respectively. The film conductivity decreased with increasing laser energy, while increasing in the the activation energy of In_2O_3 nanopartical.

Keywords: Indium Oxide, thin films, Pulse Laser Ablation, Laser energy.

الخصائص التركيبية والسطحية لأغشية اوكسيد الأنديوم النانوي التركيب المحضر بتقنيه الأستئصال بالليزرالنبضي

سارية محمد[1]، وفاء خلف[1]، سرى رعد*[2]
[1]قسم العلوم التطبيقيه ، الجامعه التكنولوجيا، بغداد، العراق
[2]هيئة الرقابة الوطنية، وزارة العلوم والتكنولوجيا، بغداد، العراق

الخلاصة

في هذا البحث، تم دراسة خصائص اوكسيد الانديوم بأستخدام تقنية الأستئصال بالليزرالنبضي لمعدن الأنديوم على شكل قرص الذي وضع في وعاء كوارتز يحتوي على 3 ملليتر من الايثانول. تم دراسه تأثيرطاقة الليزر على خصائص المادة ذات التركيب النانوي من خلال قياسات حيود الاشعه السينيه(XRD)، مجهز القوة الذرية (AFM) والمطياف المرئي. من خلال فحوصات حيود الاشعة السينية اظهرت النتائج ان الاتجاهية المفضلة لغشاء اوكسيدالأنديوم كانت (222) وشدة القمة تزداد مع زيادة طاقة الليزر، وفجوة الطاقة بحدود (3.9، 3.8، 3.6) الكترون فولط لطاقات الليزر (150، 300، 500) ملي جول عالتوالي.

Introduction

The laser ablation technique was used extensively to treat compositions of nanoparticles, because of its many features, such as the easy transport of a target material composition into products at a

*Email:Suraraad98@yahoo.com

low working temperature for high-melting and multicomponent materials. Newly, various kinds of compound nanostructures quantum dots [1]. And one-dimensional nanostructures, such as nanowires [2]. Nanotubes [3]. And composite nanostructures [4]. Have been fabricated by this technique. In addition; it has been shown that size control is available by changing the laser wavelength and the laser pulse duration and additional laser irradiation of colloids [5]. The simplicity of preparation procedure of the laser ablation method gives remarkable advantage over chemical assembly. It was shown that laser ablation in liquids is applicable to prepare Nanoparticles are not only noble metals, but also composition materials [6]. In_2O_3 is a semiconductor material with a direct energy gap of about 3.6 eV [7] and an indirect energy gap of about 2.6 eV [8]. It is also used in solar cells, transparent electrodes for heterogeneous solar cells, LCDs [9, 10]. Antireflection coatings for silicon solar cells [11,12]. This research studied experimental results of the synthesis of indium oxide nanoparticles using laser ablation of a solid target in a fluid environment and demonstrates the effect laser energy on the morphology, grain size and absorption spectrum analysis of the obtained colloid nanoparticles .

Experimental part

The experimental setup for the laser ablation experiment is schematically shown in Fig. (1). The irradiation of the metal piece by focusing laser wavelength 1.064 nm. Drowned deep in the target into the solution was kept at about 0.8 cm. After ablating the indium target by laser,the color has changed to yellow indicating the production of indium oxide colloidal nanoparticles.The In_2O_3 colloids nanoparticles deposited on slides from glass (2×2) cm^2 as thin films drop casting. An atomic force microscope the nanoparticles AFM and XRD measurements have been employed for the characterization of the nanoparticle thin films. A transmission spectrum of the nanoparticles solution was measured by UV-visible (UV-VISIBLE) spectrophotometer and the Energy band gap (eV) for prepared thin films also calculated.

Figure 1-shows the PLA system.

Results and dissections

X-ray diffraction results

The X-ray diffraction patterns of the In_2O_3 nanoparticle prepared at different energies (150, 300, 500) mj and deposited on glass substrate shows in figure (2). It's clear from figure, All the X-ray diffraction patterns show a sharp hump like feature around ($2\theta = 30^\circ$) Which can be due to the random nature of the substrate or the nano-crystalline nature of the films observed in diffraction laser energy (2θ) of (30^o) corresponded to the (222) planes (preferred orientation), and the intensity of the (222) plane increases with increasing laser energy. In addition, for all energies, we observe the presence of a weak peak in all curves. These results agree with In_2O_3 (ASTM) (JCPDS: 06-0416). Structural properties (hkl) and interplaner distance of In_2O_3 nanopartical listed in the Table-1. From the X-ray diffraction the plane orientation as a function of laser energy were determined; also grain size, calculated and listed in Table-1.

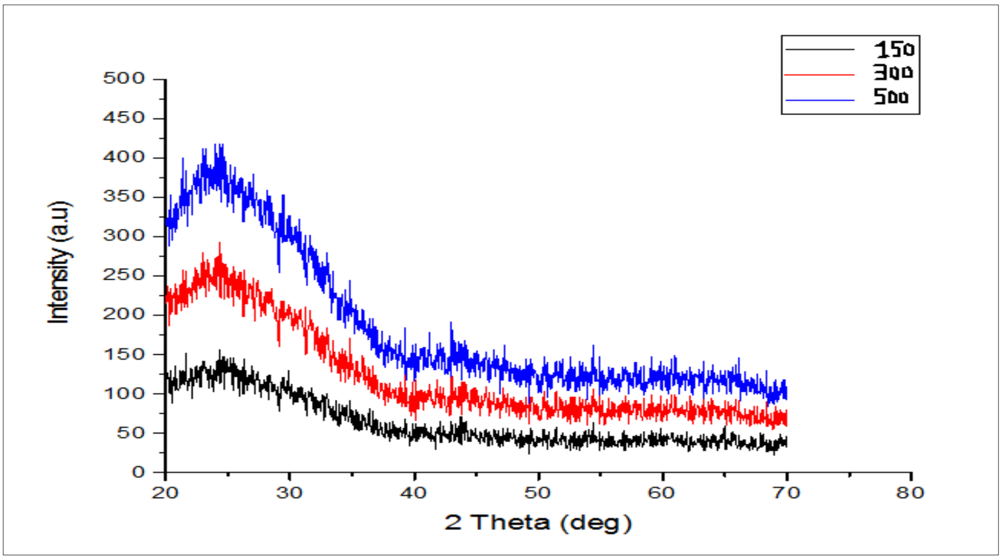

Figure 2-shows the X-ray diffraction peaks at a different laser energy of (In_2O_3) thin films (150, 300 and 500)mj.

Table 1-structural properties of (In_2O_3) thin films different laser energy

energy	h	k	l	2Θ (deg)	FWHM (deg)	d ASTM (A°)	d XRD (A°)	a ASTM (A°)	a XRD (A°)
150	3	1	0	25.184	0.2333	3.2	3.53337	10.11	11.173497
	3	2	1	33.0398	0.175	2.704	2.709	10.11	10.1361499
	2	2	2	30.6176	0.25	2.921	2.91757	10.11	10.1067589
300	3	2	1	33.0273	0.225	2.704	2.71	10.11	10.1398915
	4	0	0	35.8138	0.2133	2.53	2.50528	10.11	10.02112
	4	1	1	37.4608	0.15	2.384	2.39883	10.11	10.1773738
	4	4	0	51.7358	0.1833	1.7886	1.76554	10.11	9.98740245
500	3	1	0	25.3005	0.3666	3.2	3.51737	10.11	11.1229006
	2	2	2	30.4428	0.2	2.921	2.93392	10.11	10.163397
	3	2	1	33.6267	0.1	2.704	2.66305	10.11	9.9642207
	4	0	0	35.1065	0.3375	2.53	2.55411	10.11	10.21644
	3	3	2	41.233	0.15	2.1572	2.18766	10.11	10.2610349

From the Table-1 the lattice constant value for all samples and of the preferred orientation (222) with a lattice parameter of cubic (In_2O_3), $a^o=c^o$ = 10.1178 Å) which is in good agreement with the standard value of a = 10.11 Å [13]. While the Full Width Half Maximum gives indication of the existence of dislocations in the material [14]. It is equal to the width of the line profile (in degrees) at half of the maximum intensity from Table-1, it is clear that the Full Width Half Maximum increases with increasing laser energy; the Full Width Half Maximum of X-ray diffraction depends on the crystalline quality of each grain and distribution of grain orientation [15].

Atomic Force Microscope results

Atomic Force Microscope images Indicate changes in the surface of the film's behavior. Also us information about the average size and size distribution of the islands and provides information about the shape of the island [16]. The results provide proof that the laser energy has greater effect the final surface morphology of Indium oxide nanoparticles thin films as can be shown in Figure (3-a, b and c) for scan area (10×10) µm. Table-2 lists the particle size as a function of laser energy . Increasing the laser energy leads to increases the particle
size. Actually,increasing laser energy means delivering more energy implies ablating larger amount of material. It was noticed that increasing laser fluence produced a plasma plume
becomes more intense, and the indium oxide nanocolloidal particles could becomes denser. the values of roughness (R_a) were calculated, as it is shown in the table (2), the general output concluded is that a change in laser energy leads to change in film structure [17].

Table 2-Grain sizes of indium oxide nanoparticle film prepared at different laser energies (150, 300 and 500) mj determined from AFM scans

Laser energy (mj)	Roughness high (R_a) (nm)	Crystal size (C.s) nm
150	**1.03**	**20**
300	**2.06**	**35**
500	**11.4**	**55**

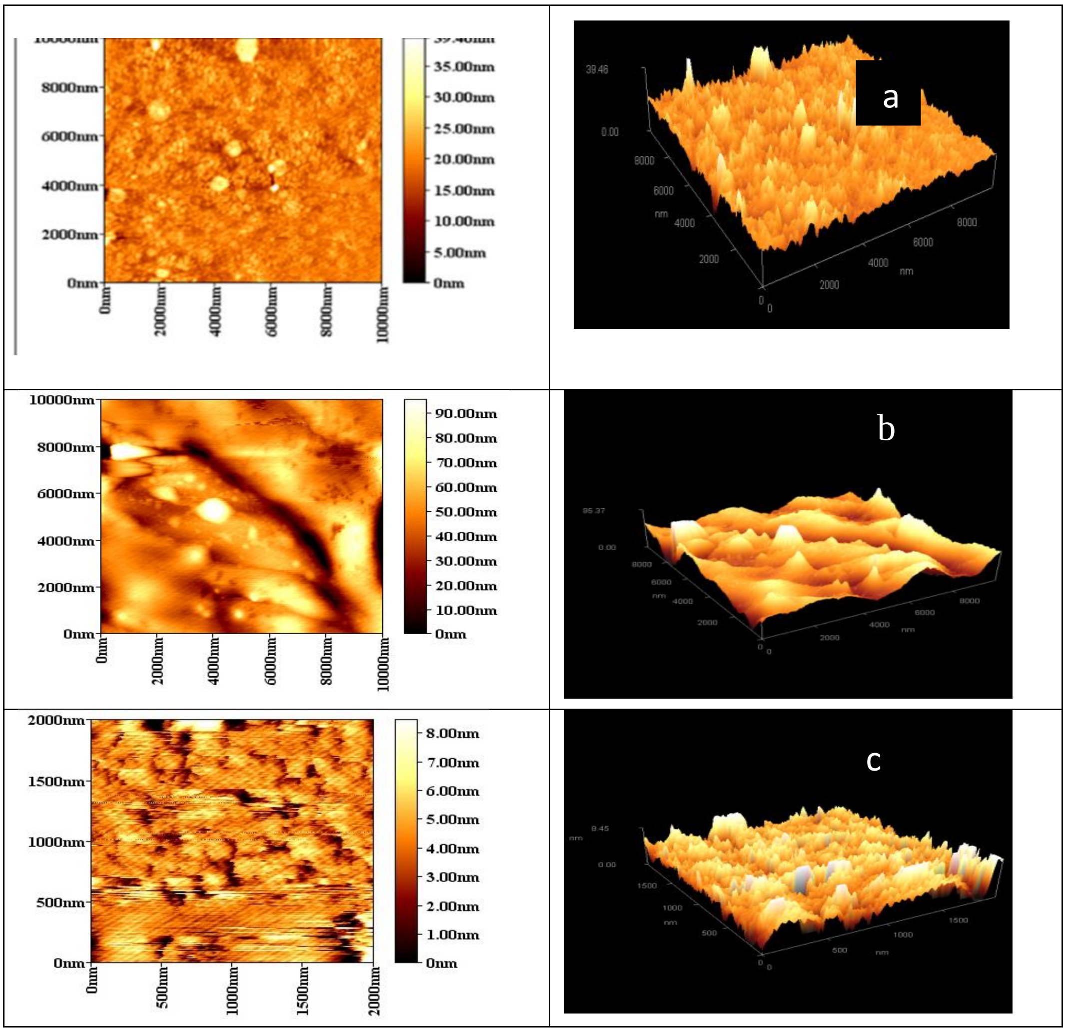

Figure 3-Atomic Force Microscope images of different laser energy at (a) 150mj, (b) 300mj and (c) 500mj.

Optical properties

UV–visible spectroscopy is one of the most widely used techniques for structural characterization of In_2O_3 NPs. shows UV–visible transmition spectra of In_2O_3 NPs, immediately after ablation, prepared by different laser energies. It has been observed in all samples, high average transmittance invisible-Nir- IR regions (window effect) and increases with both increasing wavelength and laser energy [18]. This may be ascribable to the enhancement in the crystallinity of the In_2O_3 crystallites; this improvement in the films structure and surface homogeneity.

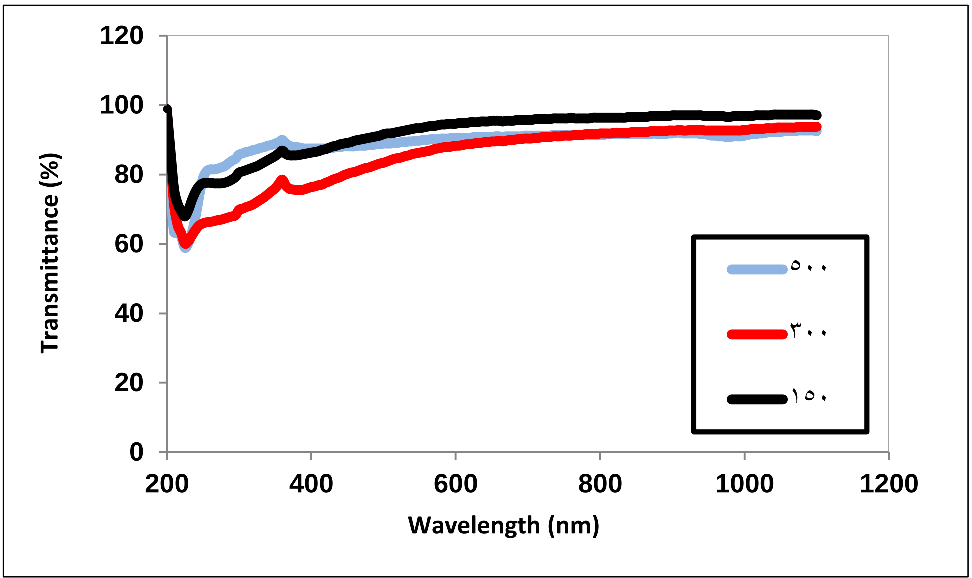

Figure 4-the relation between transmittance and wavelength of In_2O_3 nanoparticles at different laser energy (150, 300 and 500)mj.

In order to understand the optical feature of the prepared films, it is very important to study and estimate the mean value of the energy band gap which depends on the films structure, the atom arrangement and distribution in the crystal lattice [19]. The reason of making variations in energy gap is the variation in the structural properties and others, the usual technique in which the value of (E_g) can be determined, involves a plotting graph of (αhν)r versus photon energy (hν), if an appropriate value of (r) is used to linearize the diagram then the (E_g) value will be given by intercepting the (hν) axis when (αhν) r = 0 [20]. Figure (5), display the relation between $(\alpha h\upsilon)^2$ and Photon energy (hυ) of in depositing, prepared at different laser energy (150, 300 and 500) mj, it has been noticed that when the laser energy increased the band gap value increased [17]. The increase laser energy led for increasing in the film crystallize as it is previously mentioned and decreasing in the structure defects which led to increasing in energy band gap, the space between the levels in the bands becomes larger in order that the energy structure can be changed from aquatic continuous band to separate quantized levels and the band gap increases [21]. Also due to qntum confinement .Hence this effectiveness can be useful for some devices, like optical memory applications [22].

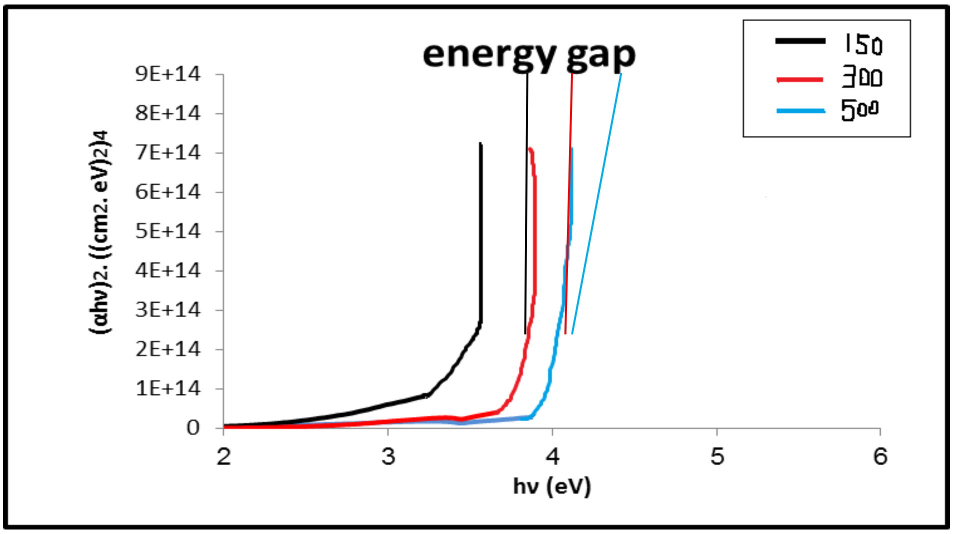

Figure 5-The relation between $(\alpha h\upsilon)^{2}$ with $(h\upsilon)$ for (In_2O_3) films deposited at different laser energy(150, 300 and 500)mj .

Electric properties

Electrical Conductivity (σ)

Figure-6 (a, b) shows the relationship between conductivity and temperature and (lnσ) vis (1000/T) of In_2O_3 nanoparticles prepared at different laser energy respectively.its clear The film conductivity decreased with increasing laser energy and temperature . From figure (6- b) the activation energy can be calculated and listed in the table (3). This result agrees with research [23]. Also, it was noticed that the value of the activation energy of In_2O_3 nanoparticles prepared at the laser energy (500) mj having higher value about (0.1656) eV as compared with the other laser energies (150) and (300) mj, as a consequence of quantum size effectiveness and the increasing in the band gap at higher laser energy.

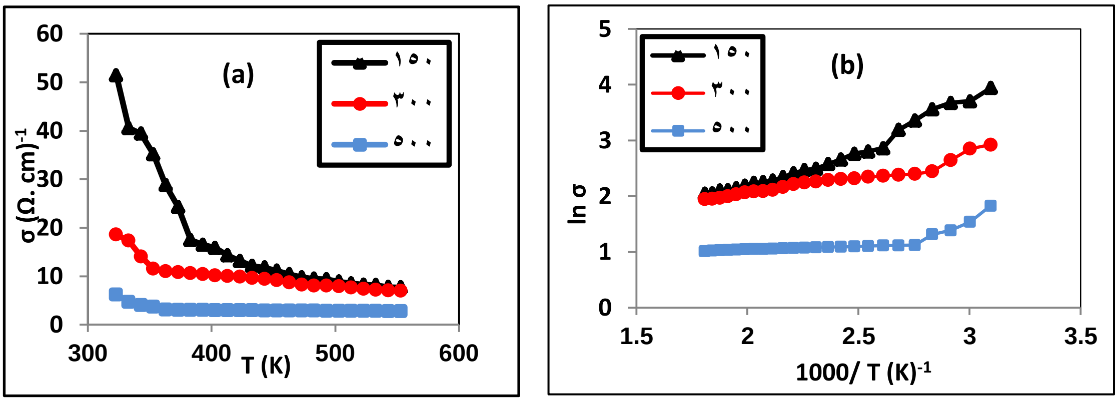

Figure 6(a, b)-show the relationship between conductivity and temperature for (In_2O_3) thin film (a) and Plots of lnσ with 1000/T of (In_2O_3) nanoparticles prepared at different laser energy (150, 300 and 500)mj .

Table 3-Shows change activation energy of In_2O_3 nanoparticles prepared at different laser energy.

Energy laser	Activity energy (E_a)
150	**0.1313**
300	**0.1467**
500	**0.1656**

Capacitance – voltage measurements (C-V)

The capacitance junction difference and $(1\backslash C^{2})$ with the reverse bias voltage for In_2O_3 nanoparticles heterojunctions that are prepared at different laser energies is shown in Figure-(7, 8) respectively, it is observed that the junction capacitance decreased with increasing the reverse bias voltage. This action is due to the width increasing in the depletion layer with increasing reverse biased voltage, and this action confirms junction formation **[24]**. Also, it's clear from the figures that the film capacitances increase with increasing laser energy. Figure-8 presents the$1/C^2$ versus reverse bias voltage plot of the heterojunction. The linear relationship indicates an abrupt junction with a 0.6 eV built-in-potential at (150)mj. Figure-8 indicates a decreasing built-in-potential of the heterojunction with the laser energy increase.

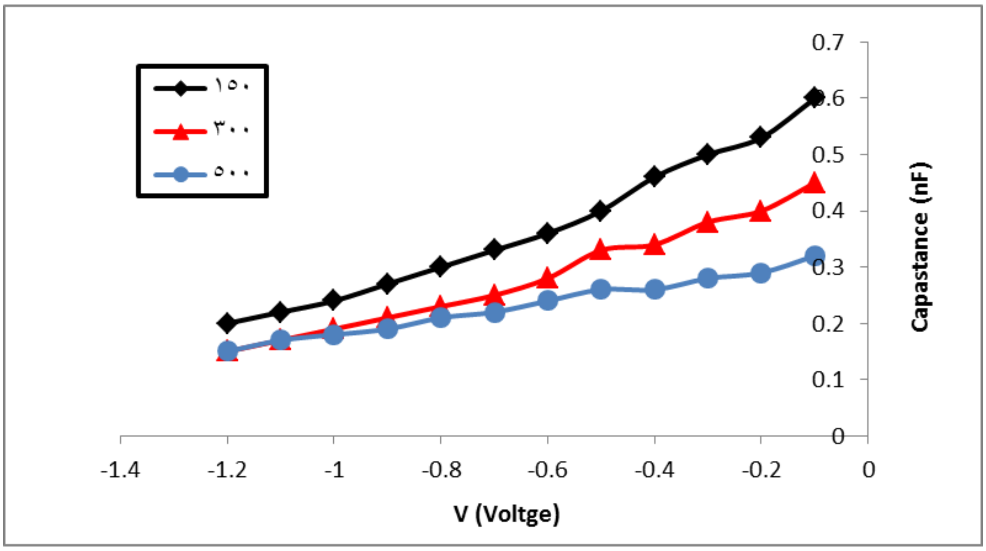

Figure 7-shows Effect of laser energy on C-V characteristics of In_2O_3nanoparticles heterojunction (150mj, 300mj and 500mj).

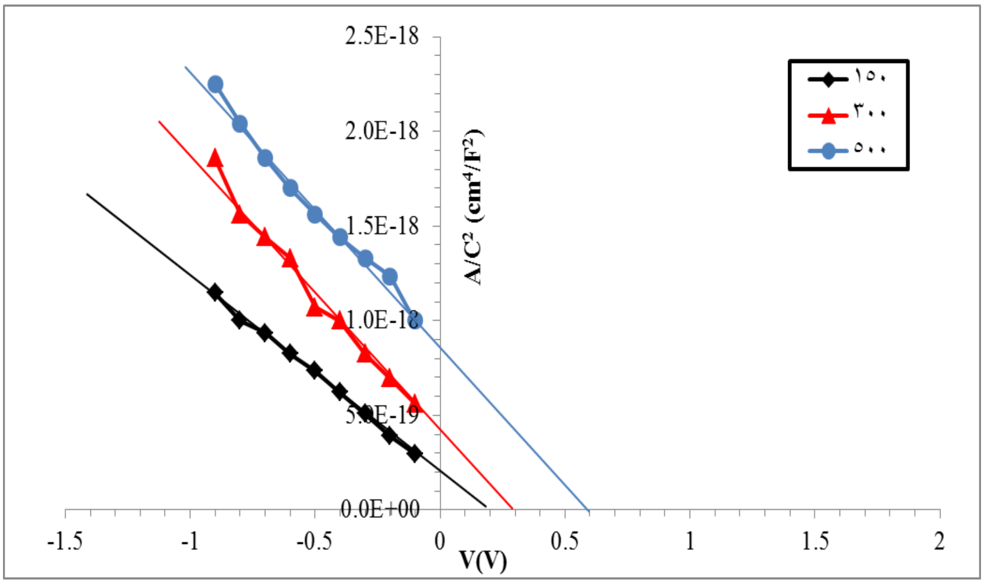

Figure 8-shows the relationship of ($1/C^2$–V_{bi}) of In_2O_3 nanoparticles heterojunction at different laser energy (150, 300 and 500)mj.

Conclusions

In closing, we have presented an experimental study of the indium oxide (In_2O_3) nanoparticles using pulse laser ablation (PLA). The outcomes indicate that all the films having preferential orientation along (222) plane and intensity increases with increasing laser energy. While The atomic force microscope images of the indium oxide nanoparticles reveal the formation of a porous granular surface, and the surface roughness values are in the range between 20 nm and 55 nm . transmittance increasing with both increase the laser energy and wavelength,and the energy gap increased with increasing laser energy. The film conductivity decreased with increasing laser energy, led to activation energy increased .

References

1. Wensheng, Sh. **1999.** "Nonlinear Optical Properties of Self-Organized Complex Oxide Ce:$BaTiO_3$ Quantum Dots Grown by Pulsed-Laser Deposition" *Appl. Phys. Letts*., 75:1547–49.
2. Morales, A.M. and Lieber, C.M. **1998.** “A Laser Ablation Method for the Synthesis of Crystalline Semiconductor Nanowires” *Science* (Washington, DC), **279**: 208–11(1998).
3. Lee, R.S., Kim, H.J., Fischer, J.E., Thess, A. and Smalley, R.E. **1997**. “Conductivity Enhancement in Single-Walled Carbon Nanotube Bundles Doped with K and Br” ‹*Nature* (London), **388**: 255–57.
4. Zhang, Y., Suenaga, K., Colliex, C. and Iijima, S. **1998.** “Coaxial Nanocable—Silicon Carbide and Silicon Oxide Sheathed with Boron Nitride and Carbon” *Science* (Washington, DC), **281**: 973–75.
5. Bulgakova, N.M. et al. **2010.** Formation of microtower structures on nanosecond laser ablation of liquid metals**.** *Appl. Phys. A*, **98**: 393-400.
6. Niedzielski, P. and Siepak, M.. **2003.** Analytical methods for determining arsenic, antimony and selenium in environmental samples.*Polish J Env. Studies*, **12**(6): 653-667.
7. Rupprecht, G. **1954.** "Untersuchungen der elektrischen und lichtelektrischen Leitfähigkeit dünner Indiumoxydschichten". *Z. Phys***,** Volume 139, Issue 5, pp 504–517.
8. Weiher, R. L., Ley, R.P.. **1966.** Optical Properties of Indium Oxide. *Journal of Applied Physics*, 37(1):.299-302.
9. Sreenivas, K. Rao, S. T. And Mansingh, A. **1998**. Preparation and characterization of rf sputtered indium tin oxide films. *J. Appl. Phys*. **57**(2): 384-392.
10. Shigesato,Y. Thalaki, S. And Haranob, T. **1992.** Electrical and structural properties of low resistivity tin-doped indium oxide films. *J. Appl. Phys*. **71**: 3356-3364.
11. Beena, D., Lethy,K.J., Vinodkumar, R. and Mahadevan Pillai V.P. **2007.** Influence of substrate temperature on the properties of laser ablated indium tin oxide films, Solar Energy Materials and *Solar Cells*, **91**(15-16): 1438-1443.
12. Salehi, A. **1998.** The effects of deposition rate and substrate temperature of ITO thin films on electrical and optical properties.*Thin Solid Films*, **324**(1-2): 324 214.
13. JCPDS Card No. 06-0416, JCPDS International Center for Diffraction Data, Swarthmore, USA.
14. Newhouse, P.F. et.al. **2005.** "High electron mobility W-doped In_2O_3 thin films by pulsed laser deposition" Appl. Phys. Lett. 87, 112108.
15. Cullity B.D. **1978.** *Elements of X-ray Diffraction*, 2nd Ed., Addison Wisely, London.
16. Cotton, F.A., Wilkinson, G., Murillo, C.A. and Bochmann, M. **1999**. *In Advanced Inorganic Chemistry*, John Wiley & Sons.
17. Makram A.Fakhri and Sarmad Fawzi Hamza **2013.** "Nano and Micro Indium Oxide Structure Prepared Using Laser Ablation Method" *The Iraqi Journal For Mechanical And Material Engineering*, **13**(1).
18. Ali A. Yousif and Zainab S. Mahdi. **2015**. "Study the effect of irradiation by laser-ray on the optical properties of the nanostructure In_2O_3 thin films" *Eng. &Tech.Journal*,.**33 Part (B)**(5).
19. Hussain R. K., **2006**. “Prepare and study properties of polymer with semiconductor”, Thesis in Applied physics Sciences in the School of Applied Sciences of the University of Technology.
20. Chaffar Akkari F. et.al. **2007**. "Growth and properties of the $CuInS_2$ thin films" Materials Science and Engineering, Cxx.
21. Beenaa, D. **2009.** "Effect of substrate temperature on structural, optical and electrical properties of pulsed laser ablated nanostructured indium oxide films". *Applied Surface Science*, **255**(20): 8334-8342.
22. Carlson, D.E. and Wronski, C.R. **1979.** "*Amorphous semiconductors*", Sepringer-Verlag, Berlin (1979).
23. JolantaStankiewicz et.al. **2017** "Structural and electrical properties of indium oxide thin films grown by pulsed laser deposition in oxygen ambient" *Journal of Alloys and Compounds*, **694** : 1280-1286.
24. Ayouchi, R. **2009.** "Photosensitivity of Nanocrystalline ZnO Films Grown by PLD", *Applied Surface Science*. **255**(11): 5917-5921.